Inter-ELM Pedestal Evolution and the Role of Edge Fluctuations in the C-Mod and DIII-D Tokamaks

A. Diallo[1], R.J. Groebner[2], J.W. Hughes[3], T.L. Rhodes[4], S.-G. Baek[3], B. LaBombard[3], J.L. Terry[3] , I. Cziegler[5], J. Walk[3], A.E. Hubbard[3], D. Smith[6], T.H. Osborne[2], J.M. Canik[7], W. Guttenfelder[1], P.B. Snyder[2], and the Alcator C-Mod and DIII-D Teams

[1] *Princeton Plasma Physics Laboratory, P.O. 451, Princeton, NJ, USA*

[2] *General Atomics, P.O. Box 85608, San Diego, CA, USA*

[3] *MIT Plasma Science and Fusion Center, Cambridge, MA, USA*

[4] *Physics Department., University of California Los Angeles, Los Angeles, CA, USA*

[5] *University of California San Diego, 9500 Gilman Dr., La Jolla, CA, USA*

[6] *University of Wisconsin-Madison, 1500 Engineering Dr., Madison, WI, USA*

[7] *Oak Ridge National Laboratory, P.O. Box 2008, Oak Ridge, TN, USA*

Understanding the physics leading to the recovery of the edge transport barrier following edge-localized-modes (ELM) crashes and buildup to the next ELM crash is an active and critical area of edge physics research for ITER projections. In one of the hypotheses of the EPED model [1], the pedestal pressure profile in H-mode discharges is predicted to be limited by micro-instabilities. One such micro-instability is the kinetic ballooning mode (KBM), which is hypothesized to provide a "soft" limit that regulates the edge transport, thereby restricting the local pressure gradient. Experiments were recently performed on the C-Mod and DIII-D devices to search for instabilities correlated with the pedestal evolution between ELMs [2, 4, 3].

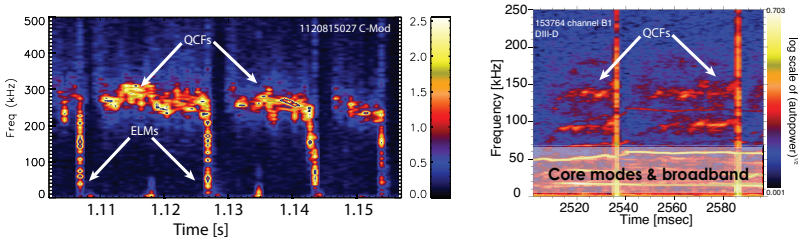

Figure 1: Magnetic spectrograms. Left panel: C-Mod (see Ref. [2]).Right panel DIII-D (see Ref. [3]).

Dedicated ELMy discharges were obtained on C-Mod with $B_T = 5.4$ T and the plasma current set at 0.9 MA in LSN magnetic configuration and high triangularity ($\delta \sim 0.8$). On DIII-D the ELMy discharges were obtained at $B_T = 1.9$T for three sets of plasma currents (0.75, 1.0, 1.6 MA). These experiments were targeted at capturing the pedestal recovery after an ELM crash using the recently upgraded Thomson scattering system on DIII-D [5]. To accurately resolve the inter-ELM dynamics, the lasers were fired in a bunch mode, which enabled temporal resolution of up to 100 μs. This increase in temporal

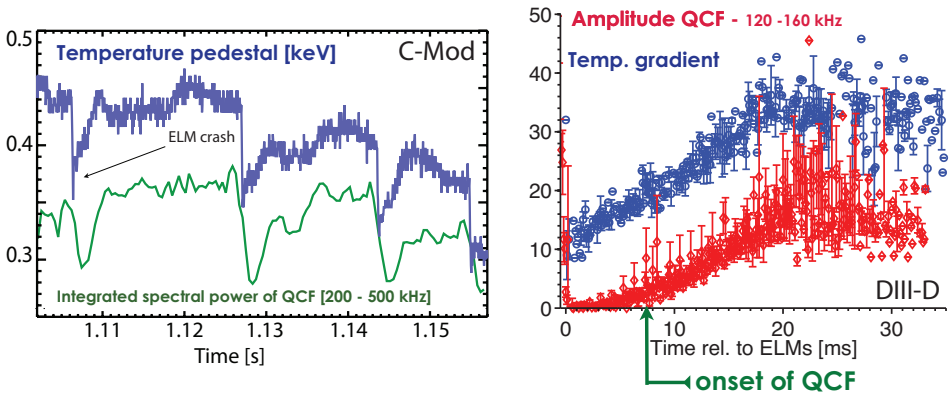

Figure 2: Left panel - C-Mod: the pedestal temperature is plotted in blue, and the integrated spectral power of the QCF is displayed in green [2, 4]. Right panel - DIII-D: the red symbols represent the amplitude of the QCF as a function of time relative to an ELM. The blue symbols display the corresponding temperature gradient evolution [3].

resolution is achieved by using multiple lasers in the same path with pulses interleaved closely in time.

Measurements of the pedestal recovery following ELMs on C-Mod and DIII-D reveal new evidence that fluctuations play an important role in the saturation of the edge gradient in the inter-ELM period. Identification of edge quasi-coherent fluctuations (QCFs) on multiple diagnostics is observed when the pressure gradient in the edge pedestal region of the plasma saturates following the ELM. Figure 1 displays the spectrograms of the magnetic fluctuations on both machines. The left panel represents the spectrogram as measured on C-Mod. The right panel of this figure displays the spectrogram on DIII-D, which indicates multiple QCFs. The lower frequencies (below 50 kHz) show core modes and broadband fluctuations uncorrelated with the ELM events. On C-Mod and DIII-D, the QCFs are observed to precede the ELM onset. The QCFs disappear after the ELM crash and later appear leading up to the next ELM.

Correlations between the QCF's onset and the pedestal parameters are shown in figure 2. On the left panel of this figure, the C-Mod results are shown, which display the temperature pedestal evolution and the integrated spectral power from the magnetic fluctuations to highlight the correlation between the onset of the QCFs and the pedestal temperature. Such correlation is clearly seen on the DIII-D results displayed on the right panel of figure 2. This panel captures the pedestal gradient evolution until saturation. At near 10 ms after the ELM crash, the QCF is observed and grows until saturation, which appears to occur nearly at the same time as the temperature gradient saturation. While causality is difficult to prove at this stage, it is suggested that the QCFs onset at a given temperature gradient and the amplitude of the QCF grows until sufficient transport is provided to clamp the gradient evolution. Coincidentally, this saturation corresponds

to the saturation of the QCF's amplitude.

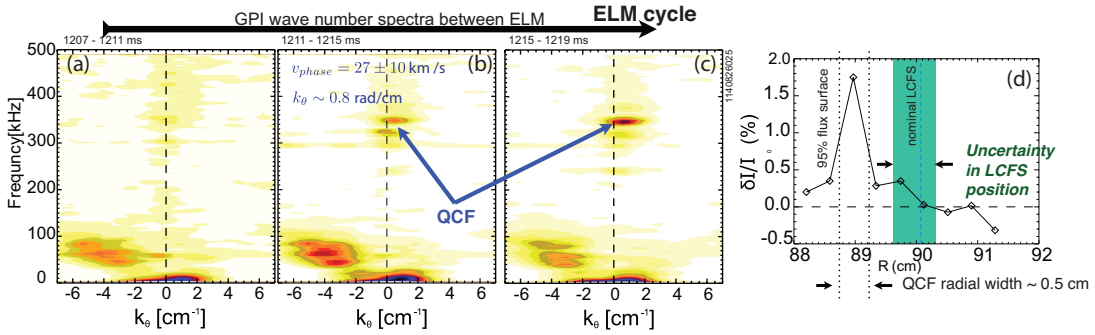

Figure 3: QCF spectral power evolution and localization using GPI on C-Mod. (a) - (c) represent the wavenumber - frequency spectrum during the inter-ELM phase on C-Mod. (d) The QCF radial profile is determined using GPI and the peak appears to be in the pedestal (see Ref [4] for details.)

The localization of the QCFs has been determined on C-Mod using the density fluctuations from the reflectometer system (see ref. [2]) as well as the GPI system. Figure 3(a)-(c) displays the GPI wavenumber frequency spectra during the the ELM cycle. Early in the ELM cycle, no QCF can be observed. Late during the ELM cycle, however, QCFs with poloidal wavenumber $k_\theta \sim 0.8$ rad/cm propagating at $v_{phase} \sim 27 \pm 10$ km/s emerge. The localization of the QCFs is indicated in figure 3(d). In this figure, the QCF is shown to be localized in the pedestal region. On DIII-D, figure 4 displays three spectrograms of the BES signals spanning the pedestal region. The location where the BES spectrograms were performed are labelled on figure 4(d). The spectrograms of the density fluctuations from BES indicate that the QCFs fluctuations appear to be localized in a narrow region of the pedestal.

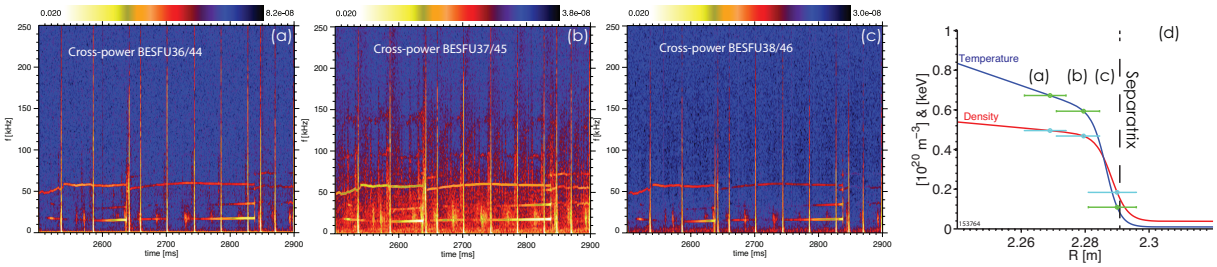

Figure 4: QCF spectral power evolution and localization using BES on DIII-D. (a) - (c) display the cross-power spectrograms at three radii, which is keyed in (d) on the temperature and density profiles [3].

Initial linear microstability properties of these edge plasmas have been analyzed for the high current case using the initial value gyrokinetic code GS2 [6]. To get an idea what kind of microinstabilities are likely to be responsible for driving the turbulence for our nominal parameters in various β regimes, linear gyrokinetics calculations in the pedestal region in C-Mod and DIII-D are performed, as displayed in figures 5 (a) and (b). Figure 5 (a) shows that the most unstable mode at low k peaks at values of $k_\theta \rho_s \sim 0.04$, which is in agreement with experimental observations on C-Mod. This low-k mode is predicted to

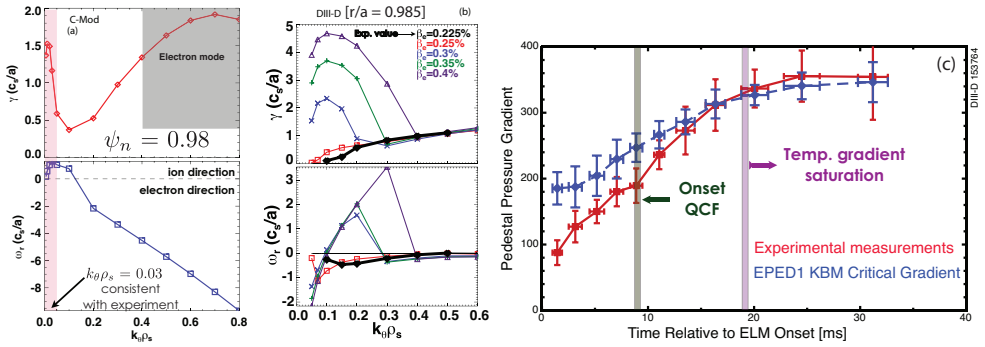

Figure 5: Left and middle panels display the results of GS2 calculations in the pedestal on C-Mod [4] and DIII-D [3]. The top of these panels are the growth rates and the bottom plots are the real frequencies. The right most panel shows the dynamic of the pedestal using EPED1 calculations. Overlaid on this plot are the time of the onset of the QCF and time when the temperature gradient saturates.

propagate in the ion direction. On DIII-D, the linear stability analysis predict an electron directed mode as shown in figure 5(b) at $\beta_e \sim 0.25\%$ slightly larger than β_e^{exp}. A β scan further indicates that at the pedestal top the most unstable mode is near KBM criticality. The propagation direction, on the other hand is predicted to be in the electron direction.

Figure 5(c) displays the gradient evolution against the time relative to an ELM. In this figure, the red squares indicate the binned averages of experimental data. From each of the data points, the EPED1 model requires eight input parameters, (B_T, I_p, R, a, κ, δ, global β, and n_e^{ped}) from which it outputs the pedestal pressure height and width (see Ref. [7] for further details). Here, given that experimental observations give fast measurements of n_e^{ped} and T_e^{ped}, the pressure pedestal is approximated by $2n_e^{ped}T_e^{ped}$ to track the dynamics. In figure 5(c), the closed blue symbols represent the EPED1 KBM constraint. EPED1 model indicates that pedestal pressure gradient reaches approximately the KBM critical gradient when the fluctuations are observed (as indicated by the green vertical line). In addition the EPED1 model predicts saturation of the pressure gradient, i.e., the observed gradient does not exceed the prediction after the onset of the instability. Overall, the QCFs on DIII-D and C-Mod appear to be consistent with the characteristics of KBM.

Work supported by the U.S. Department of Energy under DE-AC02-09CH11466, DE-FC02-04ER54698, DE-FC02-99ER54512, DE-FG02-08ER54984, DE-FG02-07ER54917, DE-FG02-89ER53296, DE-FG02-08ER54999 and DE-AC05-00OR22725.

References

[1] P.B. Snyder et al. *Nuclear Fusion*, 51(10):103016, 2011.
[2] A. Diallo, et al. *Phys. Rev. Lett.*, 112:115001, Mar 2014.
[3] A. Diallo et al. *Physics of Plasmas*, 22(5) 05611 , 2015.
[4] A. Diallo et al. *Nuclear Fusion*, 55(5):053003, 2015.
[5] D. Eldon et al. *Review of Scientific Instruments*, 83(10):10E343, 2012.
[6] M. Kotschenreuther et al. *Computer Physics Communications*, 88:128–140, 1995.
[7] P. B. Snyder et al. *Phys. Plasmas*, 16:056118, 2009.